Studying aerosol light scattering based on aspect ratio distribution observed by fluorescence microscope

LI LI,[1,2] XU ZHENG,[3,6] ZHENGQIANG LI,[2,7] ZHANHUA LI,[3] OLEG DUBOVIK,[4] XINGFENG CHEN,[2] AND MANFRED WENDISCH[5]

[1]*State Key Laboratory of Remote Sensing Science, Institute of Remote Sensing and Digital Earth, Chinese Academy of Sciences, Beijing 100101, China*
[2]*State Environmental Protection Key Laboratory of Satellite Remote Sensing, Institute of Remote Sensing and Digital Earth, Chinese Academy of Sciences, Beijing 100101, China*
[3]*State Key Laboratory of Nonlinear Mechanics, Institute of Mechanics, Chinese Academy of Sciences, Beijing 100190, China*
[4]*Laboratoire d'Optique Atmosphérique, Université de Lille 1/CNRS, Lille 59655, France*
[5]*Leipzig Institute for Meteorology, Leipzig University, Leipzig 04103, Germany*
[6]*zhengxu@lnm.imech.ac.cn*
[7]*lizq@radi.ac.cn*

Abstract: Particle shape is crucial to the properties of light scattered by atmospheric aerosol particles. A method of fluorescence microscopy direct observation was introduced to determine the aspect ratio distribution of aerosol particles. The result is comparable with that of the electron microscopic analysis. The measured aspect ratio distribution has been successfully applied in modeling light scattering and further in simulation of polarization measurements of the sun/sky radiometer. These efforts are expected to improve shape retrieval from skylight polarization by using directly measured aspect ratio distribution.

References and links

1. M. Wendisch and W. Von Hoyningen-Huene, "Possibility of refractive index determination of atmospheric aerosol particles by ground-based solar extinction and scattering measurements," Atmos. Environ. **28**(5), 785–792 (1994).
2. M. I. Mishchenko, L. D. Travis, R. A. Kahn, and R. A. West, "Modeling phase functions for dustlike tropospheric aerosols using a shape mixture of randomly oriented polydisperse spheroids," J. Geophys. Res. Atmos. **102**(D14), 16831–16847 (1997).
3. O. Dubovik, B. N. Holben, T. Lapyonok, A. Sinyuk, M. I. Mishchenko, P. Yang, and I. Slutsker, "Non-spherical aerosol retrieval method employing light scattering by spheroids," Geophys. Res. Lett. **29**(10), 54 (2002).
4. S. Merikallio, H. Lindqvist, T. Nousiainen, and M. Kahnert, "Modelling light scattering by mineral dust using spheroids: assessment of applicability," Atmos. Chem. Phys. **11**(11), 5347–5363 (2011).
5. Z. Li, D. Li, K. Li, H. Xu, X. Chen, C. Chen, Y. Xie, L. Li, L. Li, and W. Li, "Sun-sky radiometer observation network with the extension of multi-wavelength polarization measurements," Yaogan Xuebao **19**(3), 495–519 (2015).
6. B. N. Holben, T. F. Eck, I. Slutsker, D. Tanré, J. P. Buis, A. Setzer, E. Vermote, J. A. Reagan, Y. J. Kaufman, T. Nakajima, F. Lavenu, I. Jankowiak, and A. Smirnov, "AERONET—A Federated Instrument Network and Data Archive for Aerosol Characterization," Remote Sens. Environ. **66**(1), 1–16 (1998).
7. O. Dubovik, A. Sinyuk, T. Lapyonok, B. N. Holben, M. I. Mishchenko, P. Yang, T. F. Eck, H. Volten, O. Munoz, B. Veihelmann, W. J. van der Zande, J.-F. Leon, M. Sorokin, and I. Slutsker, "Application of spheroid models to account for aerosol particle nonsphericity in remote sensing of desert dust," J. Geophys. Res. Atmos. **111**(D11), D11208 (2006).
8. K. B. Aptowicz, R. G. Pinnick, S. C. Hill, Y. L. Pan, and R. K. Chang, "Optical scattering patterns from single urban aerosol particles at Adelphi, Maryland, USA: A classification relating to particle morphologies," J. Geophys. Res. Atmos. **111**(D12), D12212 (2006).
9. K. B. Aptowicz, Y. L. Pan, S. D. Martin, E. Fernandez, R. K. Chang, and R. G. Pinnick, "Decomposition of atmospheric aerosol phase function by particle size and asphericity from measurements of single particle optical scattering patterns," J. Quant. Spectrosc. Radiat. Transf. **131**, 13–23 (2013).

10. M. Ranzato, P. E. Taylor, J. M. House, R. C. Flagan, Y. Lecun, and P. Perona, "Automatic recognition of biological particles in microscopic images," Pattern Recognit. Lett. **28**(1), 31–39 (2007).
11. N. H. Robinson, J. D. Allan, J. A. Huffman, P. H. Kaye, V. E. Foot, and M. Gallagher, "Cluster analysis of WIBS single-particle bioaerosol data," Atmos. Meas. Tech. **6**(2), 337–347 (2013).
12. E. Hirst, P. H. Kaye, S. Saunders, D. W. Johnson, and M. A. Pickering, "Characterising atmospheric cloud particles using spatial light scattering," J. Aerosol Sci. **29**, S627–S628 (1998).
13. D. A. Healy, D. J. O'Connor, A. M. Burke, and J. R. Sodeau, "A laboratory assessment of the Waveband Integrated Bioaerosol Sensor (WIBS-4) using individual samples of pollen and fungal spore material," Atmos. Environ. **60**, 534–543 (2012).
14. K. Okada, J. Heintzenberg, K. Kai, and Y. Qin, "Shape of atmospheric mineral particles collected in three Chinese arid-regions," Geophys. Res. Lett. **28**(16), 3123–3126 (2001).
15. K. Kandler, N. Benker, U. Bundke, E. Cuevas, M. Ebert, P. Knippertz, S. Rodriguez, L. Schutz, and S. Weinbruch, "Chemical composition and complex refractive index of Saharan Mineral Dust at Izana, Tenerife (Spain) derived by electron microscopy," Atmos. Environ. **41**(37), 8058–8074 (2007).
16. K. Kandler, L. Schutz, C. Deutscher, M. Ebert, H. Hofmann, S. Jackel, R. Jaenicke, P. Knippertz, K. Lieke, A. Massling, A. Petzold, A. Schladitz, B. Weinzierl, A. Wiedensohler, S. Zorn, and S. Weinbruch, "Size distribution, mass concentration, chemical and mineralogical composition and derived optical parameters of the boundary layer aerosol at Tinfou, Morocco, during SAMUM 2006," Tellus B Chem. Phys. Meterol. **61**(1), 32–50 (2009).
17. K. Kandler, K. Lieke, N. Benker, C. Emmel, M. Kupper, D. Mullerebert, M. Ebert, D. Scheuvens, A. Schladitz, L. Schutz, and S. Weinbruch, "Electron microscopy of particles collected at Praia, Cape Verde, during the Saharan Mineral Dust Experiment: particle chemistry, shape, mixing state and complex refractive index," Tellus B Chem. Phys. Meterol. **63**(4), 475–496 (2011).
18. T. Nousiainen, M. Kahnert, and H. Lindqvist, "Can particle shape information be retrieved from light-scattering observations using spheroidal model particles?" J. Quant. Spectrosc. Radiat. Transf. **112**(13), 2213–2225 (2011).
19. A. E. Fonseca, M. E. Westgate, and R. T. Doyle, "Application of fluorescence microscopy and image analysis for quantifying dynamics of maize pollen shed," Crop Sci. **42**(6), 2201–2206 (2002).
20. I. France, A. W. G. Duller, G. A. T. Duller, and H. F. Lamb, "A new approach to automated pollen analysis," Quat. Sci. Rev. **19**(6), 537–546 (2000).
21. T. Miyakawa, Y. Kanaya, F. Taketani, M. Tabaru, N. Sugimoto, Y. Ozawa, and N. Takegawa, "Ground-based measurement of fluorescent aerosol particles in Tokyo in the spring of 2013: Potential impacts of nonbiological materials on autofluorescence measurements of airborne particles," J. Geophys. Res. Atmos. **120**(3), 1171–1185 (2015).
22. H. Lindqvist, O. Jokinen, K. Kandler, D. Scheuvens, and T. Nousiainen, "Single scattering by realistic, inhomogeneous mineral dust particles with stereogrammetric shapes," Atmos. Chem. Phys. **14**(1), 18451–18488 (2014).
23. M. Kahnert, T. Nousiainen, and H. Lindqvist, "Review: Model particles in atmospheric optics," J. Quant. Spectrosc. Radiat. Transf. **146**, 41–58 (2014).
24. F. M. Kahnert, J. J. Stamnes, and K. Stamnes, "Can simple particle shapes be used to model scalar optical properties of an ensemble of wavelength-sized particles with complex shapes?" J. Opt. Soc. Am. A **19**(3), 521–531 (2002).
25. M. Wendisch and P. Yang, *Theory of Atmospheric Radiative Transfer: A Comprehensive Introduction* (Wiley-VCH, 2012).
26. T. Nousiainen and K. Vermeulen, "Comparison of measured single-scattering matrix of feldspar particles with T-matrix simulations using spheroids," J. Quant. Spectrosc. Radiat. Transf. **79**, 1031–1042 (2003).
27. P. Koepke, J. Gasteiger, and M. Hess, "Technical Note: Optical properties of desert aerosol with non-spherical mineral particles: data incorporated to OPAC," Atmos. Chem. Phys. **15**(10), 5947–5956 (2015).
28. M. Wiegner, J. Gasteiger, K. Kandler, B. Weinzierl, K. Rasp, M. Esselborn, V. Freudenthaler, B. Heese, C. Toledano, M. Tesche, and D. Althausen, "Numerical simulations of optical properties of Saharan dust aerosols with emphasis on lidar applications," Tellus **61**(1), 180–194 (2009).
29. J. L. Deuze, M. Herman, and R. Santer, "Fourier series expansion of the transfer equation in the atmosphere-ocean system," J. Quant. Spectrosc. Radiat. Transf. **41**(6), 483–494 (1989).
30. H. G. Horváth and D. Varjú, *Polarized Light in Animal Vision* (Springer, 2004).
31. L. Li, Z. Li, K. Li, L. Blarel, and M. Wendisch, "A method to calculate Stokes parameters and angle of polarization of skylight from polarized CIMEL sun/sky radiometers," J. Quant. Spectrosc. Radiat. Transf. **149**, 334–346 (2014).
32. C. Pöhlker, J. A. Huffman, and U. Pöschl, "Autofluorescence of atmospheric bioaerosols – fluorescent biomolecules and potential interferences," Atmos. Meas. Tech. **5**(1), 37–71 (2012).

1. Introduction

Atmospheric aerosol particles are one of the most uncertain climate factors directly affecting the radiation budget of the Earth-atmosphere system and indirectly impacting on both the regional and global climate [1,2]. The uncertainty of the knowledge on aerosol properties can be attributed to a number of difficulties in aerosol remote sensing. Light scattering by non-

spherical particle in the atmosphere such as mineral dust is a major difficulty in aerosol characterization [2–4]. Considering that particle morphology is crucial to the properties of light scattered by particles, quantitative knowledge about various non-spherical aerosol shapes and shape distributions gets more attention in modeling the aerosol optical properties [4].

The ground-based CIMEL sun/sky radiometer CE318 can retrieve shape parameter of atmospheric aerosol particles based on the observations of the scattered skylight. CE318 has been widely deployed in the AErosol RObotic NETwork (AERONET) to study aerosol properties (including shape) at over 500 sites throughout the world. The new polarimetric radiometer CE318-DP has also been equipped at some stations of AERONET and most sites around China within the Sun/sky-radiometer Observation NETwork (SONET) [5, 6]. Compared with intensity, polarization of skylight resulting from interactions of unpolarized direct sunlight with atmospheric particles is more sensitive to particle shape [7]. Polarimetric measurements of sun/sky radiometer have been used to perform retrieval of the percentage of non-spherical aerosol particles. That is a simplification for the complex retrieval of shape distribution where the non-spherical particles are modeled as a mixture of spheres and spheroids with a priori fixed dust shape distribution retrieved from laboratory measurements [7]. The difference between shape distribution of natural aerosols and the priori fixed dust shape distribution still should be considered for improving the retrieval of shape parameter.

Some other optic instruments (e.g., TAOS, WIBS) fire a laser beam to a particle then analyze the spatial distribution of scattered light to rapidly obtain shape information [8–13]. They are not used in this study because the uncertainty in light-scattering calculation of non-spherical particles will exist in both the forward and retrieval processes considering that the light scattering method has been adopted by the sun/sky radiometer retrieval algorithm. Except the light scattering technology, another unique microscopy technology will be applied to directly measure the shape distribution of natural atmospheric aerosol particles. Previous studies commonly addressed aerosol shape distribution by electron microscopic single particle analysis [14–17], such as Scanning Electron Microscopy (SEM) and Transmission Electron Microscopy (TEM). An advantage of SEM/TEM is its high resolution up to few nanometers or even finer. To obtain the distribution, shape parameter (e.g., aspect ratio) should be calculated for each particle. Commonly, tens of thousands of individual particles need to be dealt with to get statistically significant results. For SEM/TEM, this process will become extremely laborious and time-consuming.

Some measurements have identified more spherical shapes for fine particles with diameter smaller than 500 nm and more elongated shapes for larger particles [16]. Usually the impact of particle shape on light scattering is investigated for coarse particles such as mineral dust since scattering by fine particles is expected to be independent of particle shape [3,7,15,16,18]. The shape distribution analysis for coarse particle dominated aerosols does not require very high resolution. Thus, the optic microscope is possible to be applied to study the shape distribution. In addition to white light image, fluorescence image can also be obtained by the optic microscope via fluorescent emission from aerosol particles excited by laser. Fluorescence microscopy has been widely used in studies of biological particles (e.g., pollen) [10,19,20]. While measurements of fluorescent particles have also shown that nonbiological aerosol particles like dust were also observed in fluorescence image owing to the existence of dust particles commonly containing polyaromatic hydrocarbons or biological materials [21]. This paper attempts to adopt the fluorescence microscope to determine aerosol aspect ratio distribution and further to apply the measured aspect ratio distribution in modeling light scattering and in simulation of skylight polarization measured by the sun/sky radiometer. The result of aspect ratio distribution measured at local station is expected to replace the priori fixed dust aspect ratio distribution in sun/sky radiometer retrieval.

2. Data and method

Natural atmospheric aerosol particles show a great variety of shapes which make it difficult to realistically model aerosol particle shapes and shape distributions. Although some complex three-dimensional shapes retrieved from the SEM images using stereogrammetry have been successfully applied to represent realistic morphologies of non-spherical aerosol particles in fundamental electromagnetic scattering study [22], the highly simplified models are more practically used in remote sensing or radiative transfer applications [23]. Non-spherical aerosol particles have been modeled by different shapes (e.g., cube, Gaussian random sphere, spheroid, axisymmetric Chebyshev particle) [18,23]. Among them, the spheroid model with a shape mixture of randomly oriented polydisperse spheroids is commonly adopted [3,7,18,23,24]. Numerous studies have indicated that spheroids have distinct advantage in simulating not only scattering phase function (F_{11}) but also other elements of the scattering matrix [25] (e.g., F_{12}, F_{22}, F_{33}) for complex non-spherical aerosol particles [7,18]. Modeling light scattering by varying the mixture of aspect ratios of spheroids enables to cover a large range of different scattering matrices, which makes it often possible to find the best-fit aspect radio distribution to match the scattering matrix of irregular non-spherical particles [18]. Therefore, the model of polydisperse randomly oriented spheroids was employed in this study.

Some studies have also shown that non-spherical particles can be assumed as prolate spheroids considering that this assumption yields to an improved agreement with measured scattering matrices compared to mixtures of prolate and oblate spheroids [26–28]. For the prolate spheroid model, particle shape is conveniently characterized by the aspect ratio ε, which is defined as the ratio of the largest to the smallest particle dimensions [7]. Then the spheroid shape distribution can be described by using the distribution of the spheroid aspect ratios $dN(\varepsilon)/d\ln\varepsilon$.

To measure the aspect ratio distribution, atmospheric aerosol samples were collected on 47 mm pure Teflon filter by a Total Suspended Particulate (TSP) sampler (Airmetrics Minivol Tactial Air Sampler) at Beijing-RADI station (40.005° N, 116.379° E, 59m), which is a joint site of AERONET and SONET located on the roof of the main building of the Institute of Remote Sensing and Digital Earth (RADI) at Beijing, China, see Figs. 1(a) and 1(b). The time for sampling was from 5:00 to 11:00 UTC on December 4, 2014, which was a typical clear day in Beijing winter. The volume air flow rate for sampling was 5 L/min. The volume flow and time of collection were controlled according to aerosol particulate matter concentrations to make sure that the samples were not overloaded.
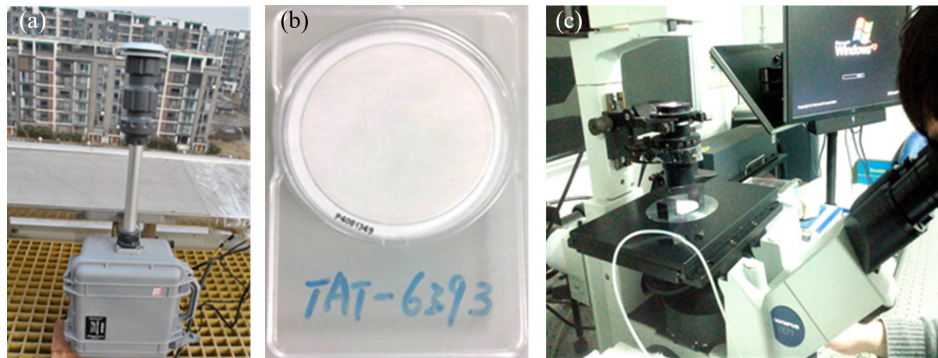

Fig. 1. Sampling and observation. (a) the Airmetrics Minivol Tactial Air Sampler, (b) 47 mm pure Teflon filter, (c) the Olympus IX71 inverted fluorescence microscope with oil- immersed 100x/1.4 objective and Andor 897 EMCCD.

An Olympus IX71 inverted microscope with oil-immersed 100x/1.4 objective and Andor 897 electron-multiplying charge-coupled device (EMCCD) was applied to obtain the images

of aerosol particle samples, see Fig. 1(c). The environment temperature in the laboratory was about 19 °C and the humidity was in the range of 15% to 20%. The samples collected on the Teflon filter were illuminated respectively by white light [Fig. 2(a)] and by blue laser at 488 nm [Fig. 2(b)]. During fluorescence observation, a long-pass barrier filter BA515 that only allows the pass of emitted light with wavelength above 515 nm was used. Images were recorded in 50 different positions which were randomly chosen on the Teflon filter surface. The exposure time of the EMCCD was 100 ms. The total size of each image was 80 μm × 80 μm with a single pixel size of about 160 nm × 160 nm. From Figs. 2(a) and 2(b), it is clear that the white-light image presents lower contract in comparison with the fluorescence image. Edges of aerosol particles are ambiguous and some ribbon shadows on the surface of Teflon filter can be found in white-light image with many fine particles sinking into them. On the contrary, the aerosol particles are clearly observed from the dark background in the fluorescence image in Fig. 2(b). By comparison, more than 95% of particles in the white-light image can still be found in the fluorescence image. Thus, the fluorescence images were adopted to identify particle shapes in following image processing. The reason why the aerosol particles can fluoresce will be discussed later in section 4. Also, we did not observe any significant quenching effect, as the grey-scale values of the particles only decreased about 10% in several minutes.
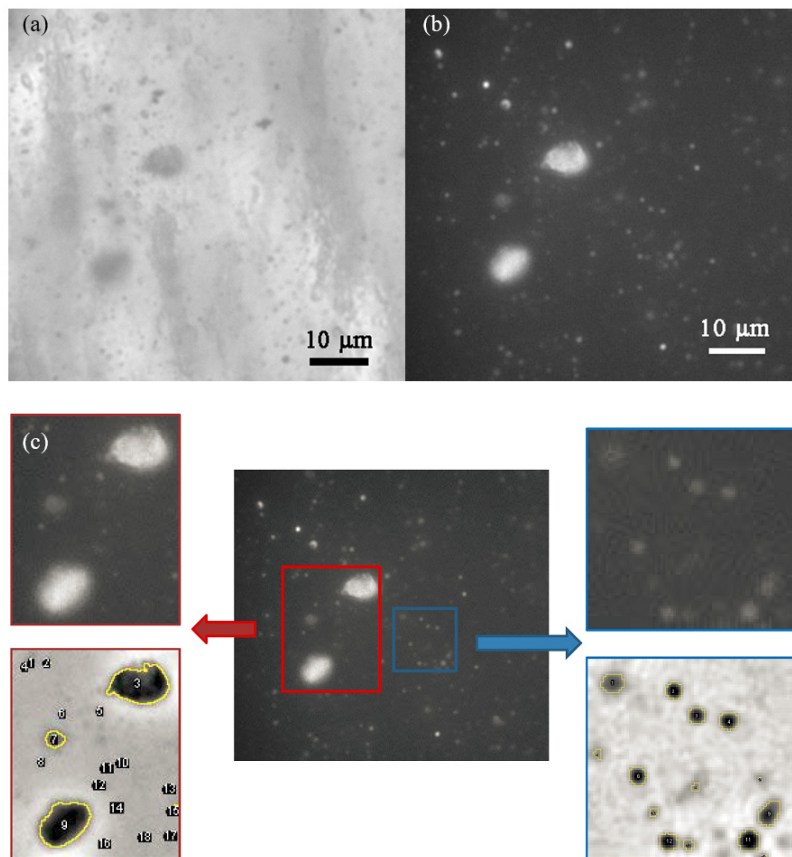

Fig. 2. Images of aerosol samples on the Teflon filter illuminated by white light (a) and illuminated by blue laser then exhibited green fluorescence (b), as well as extraction of particle shape based on the fluorescence image (c). Red box: image with coarse particles; blue box: image dominated by fine particles; yellow rings: outer edges of particles automatically extracted from the images after processing.

Fourier transform and low-pass filtering were first applied to remove background noise from the fluorescence images and to enhance the information of aerosol particles. Then, a proper threshold of grey-scale value was chosen for each image to identify the particles. The two sub-images in the lower part of Fig. 2(c) manifest the recognized particles after above processing, where the outer edges of aerosol particles were automatically extracted from the images. The grey-scale values of these two images were inverted to exhibit the high contrast and easy particle detection in the fluorescence image in comparison with the ambiguous white-light image in Fig. 2(a). It appears that either coarse particles or fine particles could be identified well by the image processing program developed in our lab based on Matlab and ImageJ. Particle inhomogeneity caused by that fluorescence sometimes originated from only a part of a particle was an issue should be paid attention, especially for coarse particles. We examined and showed that our method could recover the whole shape of the particles thanks to the high contrast in the fluorescence image, see Fig. 2(c). So, this inhomogeneity did not cause incorrect estimation of the aspect ratio. Our image processing method achieved a precision of half pixel (approximately 80 nm) on determining the particle size. By dealing with 50 fluorescence images on one Teflon filter, a total of 9537 particles were captured. The sample amount of current measurement is close to that of the previous SEM/TEM measurements [15] and thus is believed to be sufficient. Then the identified particles were fitted to spheroids and the largest to the smallest particle dimensions were measured to calculate the aspect ratios. The probability of different aspect ratios of spheroids (i.e., the aspect ratio distribution) was obtained finally.

3. Results

The aspect ratios of aerosol samples with particle surface-equivalent sphere radius from 0.2 to 10 μm (not distinguished for different sizes [7]) were determined by the fluorescence microscope. The result of the aerosol aspect ratio distribution measured at Beijing-RADI on December 4, 2014 is shown in Fig. 3(a). It was a clear sky during the sampling period. According to observations performed by the CIMEL Dual-Polar sun/sky radiometer CE318-DP at this station [5], the average aerosol optical depth (AOD) at 440 nm during this day was only 0.2. The size distribution retrieved from the CE318-DP sky measurements from 4:07 to 7:28 UTC illustrated that coarse particles were dominant during this period [7], see insert in Fig. 3(a). The measured aspect ratio distribution can be parameterized by the function given by Okada *et al.* (2001) [14] as:

$$P(\varepsilon) = \frac{2}{\frac{1}{f_1(\varepsilon)} + \frac{1}{f_2(\varepsilon)}}, \qquad (1)$$

$$f_1(\varepsilon) = 1.00561 \times 10^{-6} \exp(11.86251\varepsilon), \qquad (2)$$

$$f_2(\varepsilon) = 9.60801 \exp(-3.70901\varepsilon). \qquad (3)$$

The fitted curve is also given in Fig. 3(a). It is clear that the aspect ratio distribution measured in this study can be well fitted by this function with coefficient of determination (R^2) about 0.99.

In Fig. 3(b), the aspect ratio distributions from the literature for China (i.e., Okada *et al.*, 2001) [14], OPAC4.0 (Optical Properties of Aerosols and Clouds) mineral aerosols with r > 500 nm [27], and the distribution of Feldspar used in AERONET retrieval (i.e., Dubovik *et al.*, 2006) [7] were plotted together with the measured distribution for comparison. The distribution measured at Beijing-RADI is similar to that of Okada *et al.*, (2001) and OPAC4.0. They all rise considerably before reaching to summit then fall gradually with the increase of aspect ratios. They reach peaks at aspect ratios of 1.1 for Beijing-RADI, 1.31 for Okada *et al.*, (2001) and 1.44 for OPAC4.0, respectively. However, they show different

trends from the distribution of Dubovik *et al.*, (2006) which is dominated by the particles with aspect ratios larger than 1.44 and with a moderate increase of particle concentrations with larger aspect ratios. It is also apparent that more spherical particles measured at Beijing-RADI in comparison with other three aspect ratio distributions of mineral dust particles.
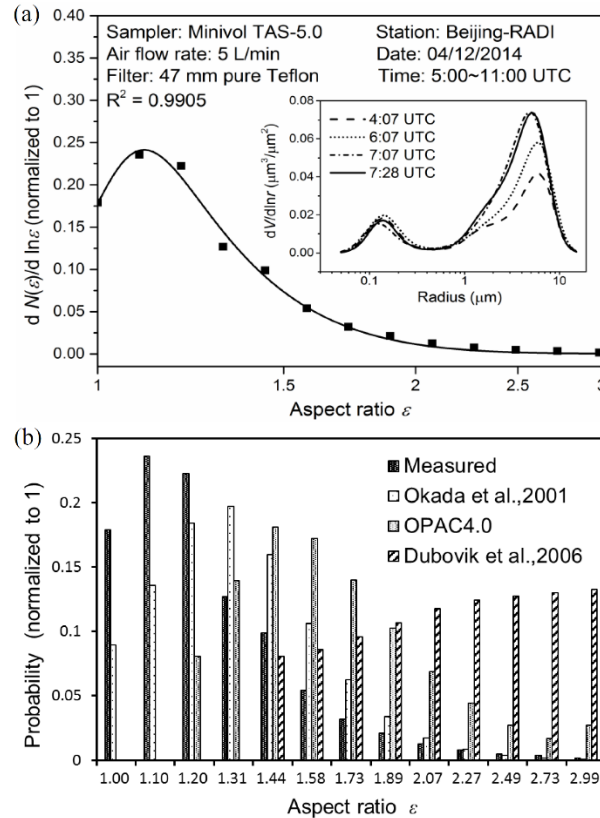

Fig. 3. Result of the measured aspect ratio distribution of aerosol particles (black squares) and the fitted curve (solid line) of this distribution (a), as well as distributions from literature for China (i.e., Okada *et al.*, 2001) [14], OPAC 4.0 mineral aerosols with r > 500 nm [27], and distribution for dust used in AERONET retrieval (i.e., Dubovik *et al.*, 2006) [7] (b).

Table 1. The median aspect radio measured at Beijing-RADI, China as well as values in literature

Sampling place	Aerosol type	Median aspect ratio	Literature
Beijing-RADI, China	Urban	1.15	this study
Qira, China	Dust	1.37,1.39	[14]
Zhangye, China	Dust	1.38, 1.41,1.42	[14]
Hohhot, China	Dust	1.32,1.37, 1.41	[14]
Izaña, Spain	Dust	1.64	[15]
Tinfou, Morocco	Dust	1.3~1.6	[16]
Praia, Cape Verde	dust, maritime	1.3~1.4 for particles smaller than 500 nm, 1.6~1.7 for larger particles	[17]

Table 1 illustrates the median aspect radio measured at Beijing-RADI as well as corresponding values given in the literature. The median aspect ratio is about 1.15 at Beijing-RADI which is lower than the values of 1.32~1.42 measured at three other Chinese arid regions reported by Okada *et al.*, (2001). Previous studies have demonstrated that the aerosol

particle shape is size dependent that reflects the chemical constituents of different types of aerosols [14–17]. A reasonable result is achieved with the samples collected in urban area in this case appearing more spherical particles than the mineral dust dominated aerosol particles collected in arid regions. Some studies have also reported that the average aspect ratio distribution of dust aerosols for China shows slightly more spherical particles than those of Saharan dust for Morocco and Cape Verde [17], as well as the long-range transport of Saharan dust at Spain [15], see Table 1. That could be attributed to more spherical particles from anthropogenic source are mixed in the Chinese samples, not only in urban area but also in arid regions. Moreover, the samples in this study were observed in laboratory condition with the humidity of 15% to 20% that was close to the natural atmospheric condition in Beijing winter. Compared with the dry samples observed in vacuum condition by SEM/TEM [14, 15], more spherical particles could be expected to be measured considering that humid situation has significant effect on water-soluble particles.
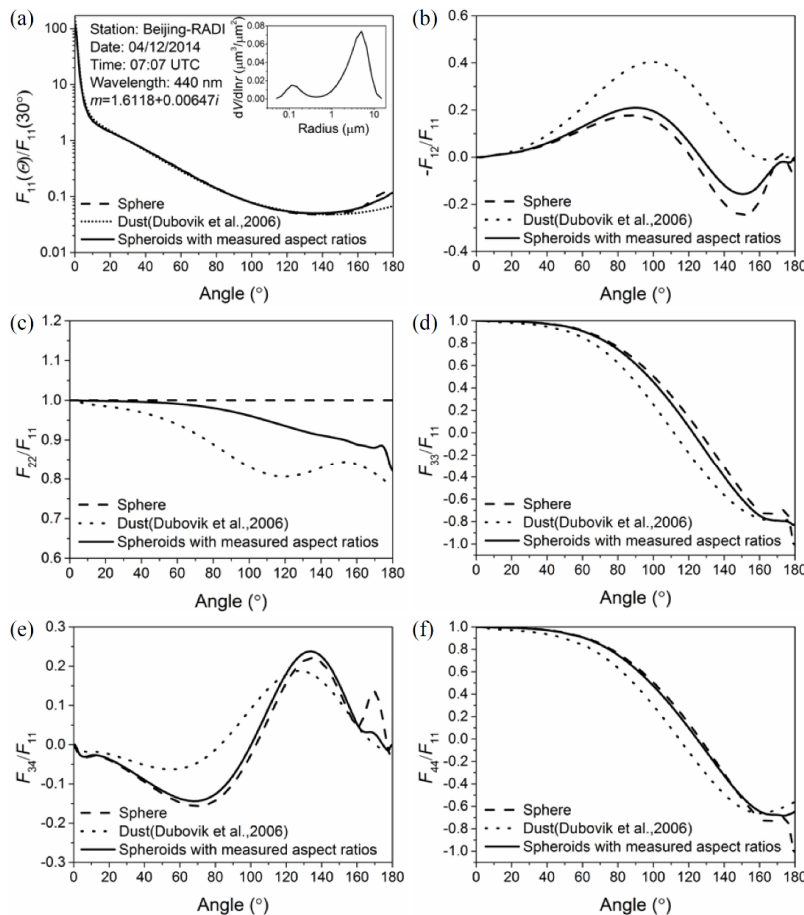

Fig. 4. Elements of the scattering matrix simulated with the measured aspect ratio distribution (solid line), sphere (dash line), and distribution of dust (dotted line) used in AERONET retrieval [7]. The particle size distribution and the complex refractive index used in simulations were retrieved from the CE318-DP sky radiance measurements at Beijing-RADI at 07:07 UTC on December 4, 2014. Wavelength $\lambda = 440$ nm. The equal presence of prolate and oblate spheroids with the same aspect ratios was still assumed for dust aspect ratio distribution as adopted in the retrieval algorithm [7], while only prolate spheroids were considered for the measured aspect ratio distribution.

The measured aspect ratio distribution was applied in modeling light scattering assuming a mixture of spheroids. Influences of different aerosol aspect ratio distributions on scattering matrix elements were simulated by the spheroid kernels software package [7]. The distribution of aspect ratios was assumed as independent of particle size in this simulation. This assumption was also adopted in the sun/sky radiometer retrieval [7]. From Fig. 4, it is obvious that elements of the scattering matrix (except F_{11}) simulated with the real-measured aspect ratio distribution are distinct from those simulated with sphere and the priori fixed aspect ratio distribution of dusts employed in AERONET retrieval [7]. The scattering phase function F_{11} changes little with aerosol aspect ratio distributions. The most obvious differences occur around the backscattering direction (i.e., scattering angles from 160° to 180°). Compared with F_{11}, other elements of the scattering matrix show significant variations with different aspect ratio distributions. These elements calculated with the real-measured aspect ratio distribution are between dust and sphere and close to the curves of sphere at the most of scattering angles from 0° to 180°. However, the sphericity parameter retrieved from the sun/sky radiometer measurements is only about 0.21% [7]. That means, non-spherical aerosol particles make up about 99.79%. This shape retrieval is conflict with the results of light scattering simulations in Fig. 4. It can be speculated that the priori fixed dust aspect radio distribution may result in a fallacious percentage of non-spherical aerosol particles.

The measured aspect ratio distribution was also applied in simulation polarization of skylight by the Successive Orders of Scattering (SOS) radiative transfer model [29], see Fig. 5. Polarization can commonly be described by the Stokes vector with four component I, Q, U, and V. Considering that the contribution of V characterizing circular polarization is negligible for the scattered skylight, skylight polarization is usually described by the first three components (i.e., I, Q, and U) [30]. The Stokes parameter U of skylight is not given because it is very close to 0 in the solar principal plane defined as the plane containing both the directions of incident sunlight and the local zenith. In comparison with the quasi-simultaneous measurements of the CE318-DP in the solar principal plane geometry, the simulated Stokes parameters I and Q show a good agreement with the measurements except for I around the solar direction and for Q in the anti-solar direction with scanning angles between 65° to 85°. The latter could be attributed to error in polarization measurements.
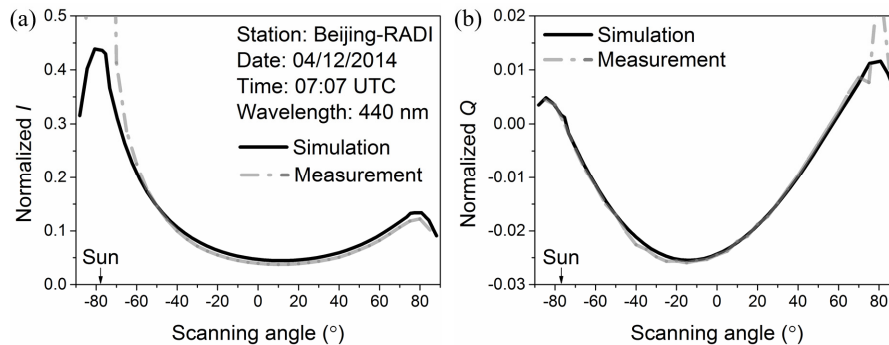

Fig. 5. Stokes parameters I and Q of skylight simulated with the aspect ratio distribution measured at Beijing-RADI (black solid line) as well as the corresponding parameters observed by the CE318-DP (grey dot dash line) in the solar principal plane geometry [31]. I and Q are normalized by the extraterrestrial solar irradiance. The particle size distribution and the complex refractive index for simulation were same as in Fig. 4. Wavelength $\lambda = 440$ nm.

4. Discussion

The reason why many aerosol particles can fluoresce is not clear yet. It is probably due to that the particles suspended in atmosphere contain different biological materials [10,19,20]. Some recent papers proposed that biological materials like lysosomes might be the source of the fluorescence [32], and reported the broad wavelength range of fluorescence emission

[13,21,32]. In current measurement, we indeed observed a few particles that did not fluoresce at all. However, by comparing the fluorescence and white-light images taken at the same position, we estimated about 95% of the visible particles collected on the Teflon filter can emit fluorescence under 488 nm blue laser illumination in this study.

We chose fluorescence microscopy method to obtain aerosol aspect ratio distribution because this method is more feasible to obtain the distributions for a number of CE318 observation stations than the traditional SEM/TEM methods. For SEM/TEM, the aerosol particles should be metallically treated before being examined, for example, coated with gold. This treatment will probably result in an overestimation of particle size. As the atmospheric aerosol particles contain significant fractions of soluble materials, humidity may have an important effect on particle shape [8]. Conventional SEM/TEM requires samples to be analyzed under vacuum condition. Therefore, aerosol particles must be dried before analysis. Even for environmental SEM, the samples are observed in low-pressure conditions then also cannot maintain their natural states in the atmosphere. However, the metallic treatment and vacuum condition are not required for the fluorescence microscope observations. Aerosol samples are observed in a temperature and humidity controlled laboratory environment (closer to their natural existing states) without any pretreatment. Moreover, less time-consuming thus ensures sufficient statistics of a large number of particles as a result of proper resolution of aerosol fluorescence-microscopy image. Nevertheless, there are still some technical issues to be improved for this method. For example, some other techniques like super-resolution microscopy are needed to overcome optical resolution and better identify fine particles with radius less than 300 nm; Chemical compositions of the particles cannot be analyzed simultaneously by this method; In addition, the white-light image also should be analyzed for some types of aerosol samples that do not exhibit fluorescence.

5. Conclusions

The aerosol shape and shape distribution play important roles in light scattering and radiative transfer in the atmosphere. Fluorescence microscopy observation in conjunction with total suspended particulate sampling was developed to determine the aspect ratio distribution of atmospheric aerosol particles. A reasonable result is achieved with the samples collected in the coarse mode particle dominant urban case. It appears more spherical particles than the mineral dust aspect ratio distribution that could be attributed to more spherical particles from anthropogenic source are mixed in the Chinese samples. This result has a similar distribution pattern with that of the electron microscopic analysis. The measured aspect ratio distribution of spheroids has been applied in modeling light scattering and further in simulation of skylight polarization. The Stokes parameters I and Q simulated with the measured aspect ratio distribution are in good agreement with the quasi-simultaneous measurements of the CE318-DP. It is evident that the aspect radio distribution determined by the fluorescence microscopy method can be successfully applied in the forward model and has high potential to be employed in the sun/sky radiometer retrieval.

The fluorescence microscopy is a feasible and practical method to obtain the aspect ratio distribution of atmospheric aerosol particles at different observation stations. More aerosol samples will be collected in northern and western China to determine the distributions of mineral dusts. The aspect ratio distributions for different radius ranges will also be discussed in future studies. These efforts are expected to replace the priori fixed dust aspect ratio distribution in current sun/sky radiometer algorithm by the real-measured aspect ratio distribution of non-spherical aerosols to improve the retrievals of aerosol shape parameters in subsequent studies.

Acknowledgments